Nonvolatile resistive switching memory based on amorphous carbon

F. Zhuge,[1] W. Dai,[1] C. L. He,[1] A. Y. Wang,[1] Y. W. Liu,[1] M. Li,[1] Y. H. Wu,[2] P. Cui,[1] and Run-Wei Li[1,a)]

[1]*Ningbo Institute of Materials Technology and Engineering (NIMTE), Chinese Academy of Sciences (CAS), Ningbo 315201, People's Republic of China*

[2]*Department of Electrical and Computer Engineering, National University of Singapore, Singapore 117576*

(Received 22 January 2010; accepted 30 March 2010; published online 21 April 2010)

Resistive memory effect has been found in carbon nanostructure-based devices by Standley *et al.* [Nano Lett. **8**, 3345 (2008)]. Compared to nanostructures, hydrogenated amorphous carbon (*a*-C:H) has much more controllable preparation processes. Study on *a*-C:H-based memory is of great significance to applications of carbon-based electronic devices. We observed nonvolatile resistance memory behaviors in metal/*a*-C:H/Pt structures with device yield 90%, ON/OFF ratio >100, and retention time $>10^5$ s. Detailed analysis indicates that the resistive switching originates from the formation/rupture of metal filaments due to the diffusion of the top electrodes under a bias voltage. © *2010 American Institute of Physics*. [doi:10.1063/1.3406121]

Resistive random access memory has attracted great attention due to its potential for the replacement of flash memory in next generation nonvolatile memory applications.[1,2] Its memory effect is realized through the switching characteristic between high resistance state (HRS) and low resistance state (LRS). The resistive switching effect was observed from various materials, such as transition metal oxides,[3–7] perovskite oxides,[8,9] chalcogenide materials,[10] and amorphous silicon,[11–13] and some carbon-based materials.[14–17] Sinitskii *et al.*[14,15] reported that two-terminal devices consisting of discontinuous 5–10 nm thin films of graphitic sheets exhibited enormous and sharp bistable current-voltage (*I-V*) behavior possessing stable, rewritable, nonvolatile, and nondestructive read memories with ON/OFF ratios of up to 10^7. Standley *et al.*[16] further presented nonvolatile memory elements based on graphene. Recently, we obtained stable nonvolatile resistive switching in graphene oxide films.[17] Given the variety of carbon materials, it will be interesting and important to develop purely carbon-based electronic devices.[18] Compared to carbon nanostructures, amorphous carbon (*a*-C) or hydrogenated amorphous carbon (*a*-C:H) has much more controllable preparation processes.[19] Therefore, study on *a*-C or *a*-C:H-based memory is of great significance to applications of carbon-based electronic devices.

In this paper, we investigated the resistive switching characteristics of *a*-C:H thin films prepared by the linear ion beam deposition technique for nonvolatile memory applications. Reliable and reproducible switching phenomena of the metal/*a*-C:H/Pt structures were observed. The mechanism of the switching effect is discussed in detail.

Hydrogenated amorphous carbon thin films of 120 nm thick were deposited on $Pt/Ti/SiO_2/Si$ substrates at room temperature (RT) by the linear ion beam deposition technique using C_2H_2 as the precursor of hydrocarbon ions.[20] The base pressure in the chamber was less than 2×10^{-5} Torr. Power of the ion gun was 250 W (0.2 A, 1250 V). The deposition pressure was maintained at 0.8×10^{-3} Torr. During the film deposition, no negative bias was applied to the substrate. In order to measure the electrical properties of the *a*-C:H films, metal top electrodes (Cu, Ag, or Au) of 100 μm in diameter were deposited at RT by electron-beam evaporation with an *in situ* metal shadow mask. The microstructure was examined by transmission electron microscopy (TEM). The atomic bonding of *a*-C:H films was studied by Raman scattering measurements using the 514.5 nm excitation from an Ar^+ laser source. The *I-V* characteristics of the metal/*a*-C:H/Pt structures were measured at RT in air using a Keithley 4200 semiconductor parameter analyzer. During the measurement in voltage sweeping mode, the positive bias was defined by the current flowing from the top to bottom electrode, and the negative bias was defined by the opposite direction. The resistances in the LRS and HRS of the metal/*a*-C:H/Pt structures were measured as a function of temperature by a physical property measurement system (PPMS, Quantum Design).

Figure 1(a) shows the cross-sectional TEM image of a-C:H/Pt/Ti/SiO_2/Si structure. It can be seen that only an amorphous granular structure with diffuse halos in the selected electron diffraction pattern was observed, as shown in the insets of Fig. 1(a). Furthermore, the hydrogenated amorphous carbon feature of the deposited film can be defined by the Raman spectrum [Fig. 1(b)], where a G-peak centered at 1525.7 cm^{-1} and a D-peak at 1350.7 cm^{-1} with an intensity ratio of I_D/I_G at 0.73 were obtained by the spectrum decon-

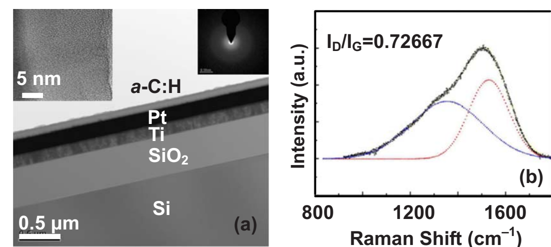

FIG. 1. (Color online) (a) Cross-sectional TEM image of the a-C:H/Pt/Ti/SiO_2/Si structure. The left panel of the insets shows a high resolution TEM image of the *a*-C:H thin film. The right one shows a corresponding selected electron diffraction pattern. (b) Raman spectrum with the deconvoluted data of the *a*-C:H film.

a)Author to whom correspondence should be addressed. Electronic mail: runweili@nimte.ac.cn.

 © 2010 American Institute of Physics

Author complimentary copy. Redistribution subject to AIP license or copyright, see http://apl.aip.org/apl/copyright.jsp

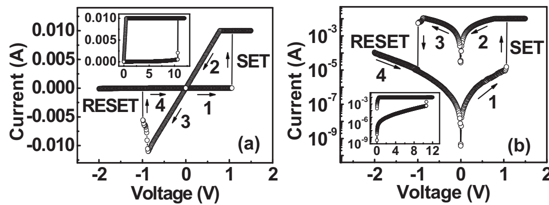

FIG. 2. Typical *I-V* characteristics of the Cu/*a*-C:H/Pt structure shown in (a) linear scale, and (b) semilogarithmic scale. The insets show the initial electroforming.

volution. Taking into account that the film was deposited without any negative substrate bias, it could be concluded that the present *a*-C:H films are of polymerlike carbon features with 35–60 at. % H and up to 70% hybridized sp^3 bonds.[21,22]

Cu/*a*-C:H/Pt sandwiched structures showed the bipolar resistive switching behavior. The *I-V* characteristics of the Cu/*a*-C:H/Pt memory cell were studied by dc voltage sweep measurements to evaluate the memory effects of the obtained devices, and the results are illustrated in both linear [Fig. 2(a)] and semilogarithmic [Fig. 2(b)] scales. The activation of the Cu/*a*-C:H/Pt memory cell requires a forming process with a current compliance (10 mA in this work, as shown in the insets of Fig. 2) as well as a forming voltage of about 10 V. After the initial forming process, the memory cell switched to the low resistance state (ON). By increasing the negative voltages imposed on the cell, a pronounced change in resistance from the LRS to high resistance state (OFF) was observed at about −1 V, which is called the "RESET" process. Subsequently, an opposite "SET" process could also be seen when sweeping the voltage reversely to positive values. The switching from the HRS to LRS occurs at about 1.1 V, and the nonvolatile switching was achieved. The SET switching must sweep with a current compliance (10 mA in this work) to protect the sample from a permanent breakdown. The Cu/*a*-C:H/Pt structures showed a high device yield of 90%.

Figure 3(a) shows the endurance characteristics of the Cu/*a*-C:H/Pt memory cell. The resistance values were read out at 0.1 V in each sweep. The resistances of the HRS and LRS scatter to a certain extent during cycling, especially for HRS. As can be seen, the memory margin keeps beyond 100 during cycling, and the cell shows little degradation after 110 repeated sweep cycles. The endurance measurements ensured that the switching between ON and OFF states is controllable, reversible, and reproducible. After the device was switched ON or OFF, no electrical power was needed to maintain the resistance within a given state. The retention performance of the memory cell at RT is shown in Fig. 4. As can be seen, the variation of LRS and HRS resistance after 10^5 s is very little, confirming the nonvolatile nature of the device.

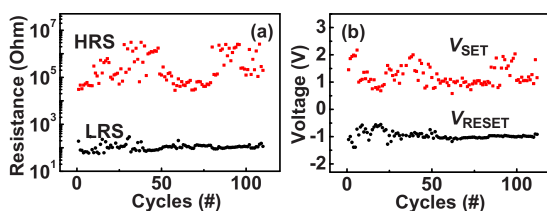

FIG. 3. (Color online) (a) Endurance performance of the Cu/*a*-C:H/Pt memory cell. The resistance values were read out at 0.1 V in each sweep. (b) Evolution of V_{SET} and V_{RESET} of the Cu/*a*-C:H/Pt device as a function of the switching cycle.

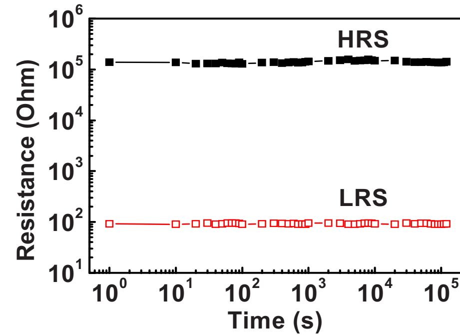

FIG. 4. (Color online) Retention performance of the Cu/*a*-C:H/Pt memory cell at RT.

To understand the conduction and switching mechanisms of the metal/*a*-C:H/Pt memory cell, the *I-V* curves were replotted in a log-log scale. Figure 5(a) shows the logarithmic plot and linear fitting of the previous *I-V* curve for the positive voltage sweep region, while it is similar for the negative branch. As shown in Fig. 5(a), the *I-V* curve of LRS exhibits a linearly Ohmic behavior with a slope of 1.01. This was thought to correspond to the formation of conducting filaments during the SET process. However, the conduction mechanisms of HRS are much more complicated. Fitting results for HRS suggest that the charge transport behavior is in good agreement with a classical trap-controlled space charge limited current (SCLC), which consists of three portions: the Ohmic region ($I \propto V$), the Child's law region ($I \propto V^2$), and the steep current increase region.[23,24] The totally different conduction behaviors in HRS and LRS also suggest that the high conductivity in ON-state cell should be a confined, filamentary effect rather than a homogenously distributed one.

Figure 3(b) illustrates the evolution of V_{SET} and V_{RESET} of the Cu/*a*-C:H/Pt memory cell within 110 switching cycles. When the cell was repeatedly switched between ON and OFF states, V_{RESET} distributes in a range of −1.2 to −0.8 V after 30 cycles, while V_{SET} shows more scattering with a wider distribution of 0.6–2.2 V. It is reported[25] that during a filament formation and rupture process, the formation of a filament (SET) should be more random than the destruction of an existing filament (RESET), since the formation process is determined by the competition among different filamentary paths. Thus one might expect larger variations in V_{SET} rather than in V_{RESET}. It might serve as another clue to the filamentary switching in our case.

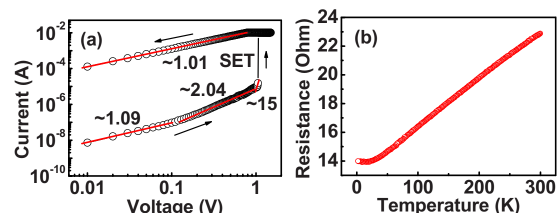

FIG. 5. (Color online) (a) *I-V* curves of the Cu/*a*-C:H/Pt memory cell plotted in log-log scale and the linear fitting results in both LRS and HRS. Also shown are the corresponding slopes for different portions. (b) Temperature dependence of the resistance in the LRS of the Cu/*a*-C:H/Pt memory cell.

Author complimentary copy. Redistribution subject to AIP license or copyright, see http://apl.aip.org/apl/copyright.jsp

The resistive switching was proposed to be filamentary in nature in the reported carbon-based devices.[14–17,26] However, the exact origin of the filament remains unclear. In our case, the bipolar resistive switching has also been observed in Ag/a-C:H/Pt and Au/a-C:H/Pt devices. It was found that the ON/OFF ratio (r) and switching threshold voltages (v) vary as follows: $r_{Cu} > r_{Ag} > r_{Au}$ and $v_{Cu} > v_{Au} > v_{Ag}$, indicating that the top metal electrode plays an important role in the switching in the present devices.[11] Briefly, a positive voltage [>SET voltage (V_{SET})] on the top electrodes generates a high electric field that drives metal (e.g., Cu) ions into the a-C:H matrix and form conducting filaments inside the a-C:H layer, and the device reaches the ON state. After the SET process, the device retains the ON state unless a sufficient voltage of opposite polarity [<RESET voltage (V_{RESET})] is applied and the electrochemical dissolution of the metal filaments RESETs the device, and the OFF state is finally reached again.[11,27] To verify the above hypothesis, the resistance in the LRS (R_{ON}) of the Cu/a-C:H/Pt device was measured as a function of temperature. Figure 5(b) shows the typical metallic behavior of R_{ON}. The metallic conducting behavior in the LRS confirms the formation of metal filaments in the a-C:H films. The temperature dependence of metallic resistance can be written as $R(T) = R_0[1+\alpha(T-T_0)]$, where R_0 is the resistance at temperature T_0, and α is the temperature coefficient of resistance. By choosing T_0 as 300 K, the α of the filaments is calculated to be 1.8×10^{-3} K^{-1}, which is similar to the value 2.5×10^{-3} for high-purity Cu nanowires of diameter ≥ 15 nm,[28] confirming that the filaments are composed of Cu in metallic states due to the diffusion of the top electrode under a bias voltage. The discrepancy of α is attributed to inevitable defects in the Cu filaments, since the presence of defects can reduce α by shortening the mean free path of electrons.[29,30] On the other hand, the resistance in the HRS was found to decrease with increasing temperature, and it exhibits a typical semiconducting behavior.

In conclusion, the reversible and steady resistive memory effect of the metal/a-C:H/Pt sandwiched structure was achieved with a resistance ratio HRS/LRS of two orders of magnitude. The Cu/a-C:H/Pt memory cells showed a device yield of 90% and a retention time of more than 10^5 s. The dominant conduction mechanisms of LRS and HRS were Ohmic behavior and trap-controlled SCLC, respectively. The observed switching effect could be attributed to the formation/rupture of metal filaments due to the diffusion of the top electrodes under an electric field.

This work was supported by State Key Research Program of China (973 Program), National Natural Science Foundation of China, the Zhejiang and Ningbo Natural Science Foundation, and Chinese Academy of Sciences (CAS).

[1]R. Waser and M. Aono, Nature Mater. **6**, 833 (2007).
[2]D. Strukov, G. Snider, D. Stewart, and R. Williams, Nature (London) **453**, 80 (2008).
[3]M. Liu, Z. Abid, W. Wang, X. L. He, Q. Liu, and W. H. Guan, Appl. Phys. Lett. **94**, 233106 (2009).
[4]Y. C. Yang, F. Pan, Q. Liu, M. Liu, and F. Zeng, Nano Lett. **9**, 1636 (2009).
[5]J. Y. Son and Y. H. Shin, Appl. Phys. Lett. **92**, 222106 (2008).
[6]W. Yang, W. Kim, and S. Rhee, Thin Solid Films **517**, 967 (2008).
[7]G. Garbarino, M. Regueiro, M. Armand, and P. Lejay, Appl. Phys. Lett. **93**, 152110 (2008).
[8]S. Q. Liu, N. J. Wu, and A. Ignatiev, Appl. Phys. Lett. **76**, 2749 (2000).
[9]A. Beck, J. G. Bednorz, C. Gerber, C. Rossel, and D. Widmer, Appl. Phys. Lett. **77**, 139 (2000).
[10]L. P. Ma, J. Liu, and Y. Yang, Appl. Phys. Lett. **80**, 2997 (2002).
[11]S. H. Jo and W. Lu, Nano Lett. **8**, 392 (2008).
[12]S. H. Jo, K. H. Kim, and W. Lu, Nano Lett. **9**, 496 (2009).
[13]S. H. Jo, K. H. Kim, and W. Lu, Nano Lett. **9**, 870 (2009).
[14]A. Sinitskii and J. M. Tour, ACS Nano **3**, 2760 (2009).
[15]Y. B. Li, A. Sinitskii, and J. M. Tour, Nature Mater. **7**, 966 (2008).
[16]B. Standley, W. Z. Bao, H. Zhang, J. Bruck, C. N. Lau, and M. Bockrath, Nano Lett. **8**, 3345 (2008).
[17]C. L. He, F. Zhuge, X. F. Zhou, M. Li, Y. W. Liu, J. Z. Wang, B. Chen, Z. P. Liu, Y. H. Wu, P. Cui, and R. W. Li, Appl. Phys. Lett. **95**, 232101 (2009).
[18]Y. M. Lin, VLSI Technol., Syst. Appl. **2008**, 74.
[19]J. Robertson, Mater. Sci. Eng. R. **37**, 129 (2002).
[20]G. S. Wu, L. L. Sun, W. Dai, L. X. Song, and A. Y. Wang, Surf. Coat. Technol. **204**, 2193 (2010).
[21]M. Shamsa, W. Liu, A. Balandin, C. Casiraghi, W. Milne, and A. Ferrari, Appl. Phys. Lett. **89**, 161921 (2006).
[22]S. Yoon, H. Yang, A. Rusli, J. Ahn, and Q. Zhang, Diamond Relat. Mater. **7**, 70 (1998).
[23]A. Lampert and P. Mark, *Current Injection in Solids* (Academic, New York, 1970).
[24]Q. Liu, W. H. Guan, S. B. Long, R. Jia, M. Liu, and J. N. Chen, Appl. Phys. Lett. **92**, 012117 (2008).
[25]Z. Wang, P. Griffin, J. McVittie, S. Wong, P. McIntyre, and Y. Nishi, IEEE Electron Device Lett. **28**, 14 (2007).
[26]Y. Naitoh, K. Yanagi, H. Suga, M. Horikawa, T. Tanaka, and T. Shimizu, Appl. Phys. Express **2**, 035008 (2009).
[27]C. Schindler, G. Staikov, and R. Waser, Appl. Phys. Lett. **94**, 072109 (2009).
[28]A. Bid, A. Bora, and A. Raychaudhuri, Phys. Rev. B **74**, 035426 (2006).
[29]A. Ioffe and A. Regel, in *Progress in Semiconductors*, edited by A. Gibson, F. Kroger, and R. Burgess (Wiley, New York, 1960), Vol. 4, p. 237.
[30]J. H. Mooij, Phys. Status Solidi A **17**, 521 (1973).

Author complimentary copy. Redistribution subject to AIP license or copyright, see http://apl.aip.org/apl/copyright.jsp